

Ginzburg-Landau functional for nearly antiferromagnetic perfect and disordered Kondo lattices

M. Kiselev,¹ K. Kikoin,² and R. Oppermann¹

¹*Institut für Theoretische Physik, Universität Würzburg, D-97074, Germany*

²*Ben-Gurion University of the Negev, Beer-Sheva 84105, Israel*

(Received 17 June 2001; revised manuscript received 28 November 2001; published 16 April 2002)

Interplay between Kondo effect and antiferromagnetic and spin glass ordering in perfect and disordered bipartite Kondo lattices is considered. The Ginzburg-Landau equation is derived from the microscopic effective action written in three mode representation (Kondo screening, antiferromagnetic correlations, and spin liquid correlations). The problem of the local constraint is resolved by means of the Popov-Fedotov representation of the localized spin operators. It is shown that the Kondo screening enhances the tendency to a spin-liquid crossover and partially suppresses antiferromagnetic ordering in perfect Kondo lattices and spin glass ordering in doped Kondo lattices. The modified Doniach diagram is constructed, and possibilities of going beyond the mean-field approximation are discussed.

DOI: 10.1103/PhysRevB.65.184410

PACS number(s): 75.20.Hr, 71.27.+a, 75.10.Nr, 75.30.Mb

I. INTRODUCTION

The Kondo lattice (KL) systems are famous for their unusual electronic and magnetic properties, including giant effective masses observed in thermodynamic and de Haas-van Alphen measurements,¹ unconventional superconductivity,² and a fascinating variety of magnetic properties.³ The great majority of the metallic KL systems demonstrates antiferromagnetic (AFM) correlations and all types of the AFM order may be found in these compounds. There are localized spins in U_2Zn_{17} , UCd_{11} , $CeIn_3$,³ quadrupole ordering in CeB_6 ,⁴ interplay between localized and itinerant excitations in several U- and Ce-based compounds,⁵ puzzling magnetic order of tiny moments in UPt_3 , URu_2Si_2 , UNi_2Al_3 ,⁶ quantum phase transition in $CeCu_{6-x}Au_x$,⁷ fluctuation-type dynamical ordering in $U(Pt_{1-x}Pd_x)_3$,⁸ short-range magnetic correlations in the astonishingly wide temperature interval of critical behavior in $CeCu_6$ and $CeRu_2Si_2$.⁹ This list is by no means exhaustive. The superconducting state in most cases coexists with antiferromagnetism, and, apparently, Cooper pairing itself is mediated by magnetic fluctuations.^{2,10} The dominant contribution to the low-temperature thermodynamics is also given by spin degrees of freedom.^{11,12}

On the other hand, all low-temperature characteristics of KL's are determined by a Kondo temperature T_K . These characteristics are Fermi-like, but the energy scale of the "fermion" spectrum is renormalized by a factor T_K/ε_F relative to a conventional electron Fermi liquid.³ Apparently, the AFM correlations due to Ruderman-Kittel-Kasuya-Yosida (RKKY) interaction I partially suppressed by intrasite Kondo effect should be treated as a background for all unusual properties of Kondo lattices. The main theoretical challenge is to find a scenario of crossover from a high-temperature regime of weak interaction (scattering) between localized spins and conduction-electron Fermi liquid to a low-temperature strong-coupling regime where the spins lose their localized nature and are confined into an unconventional quantum liquid involving spin degrees of freedom of conduction electrons.

In the phase diagram of the disordered KL more exotic possibilities such as non-Fermi-liquid regimes arise, which were observed, for example, near the $T=0$ quantum critical

point in $Y_{1-x}U_xPd_3$ (see, e.g., Ref. 13). In this family of ternary alloys the spin-glass (SG) behavior was discovered in a U concentration range $0.3 < x < 0.5$ with a freezing temperature T_f growing monotonically with x (see Ref. 14). Among other U-based heavy fermion compounds with SG behavior, URh_2Ge_2 ,¹⁵ $U_2Rh_3Si_5$,¹⁶ and U_2PdSi_3 (Ref. 17) should be mentioned. The effects of "Kondo disorder" were reported for $UCu_{5-x}Pd_x$ in Ref. 18. Later on the competition between RKKY and Kondo exchange for disordered Ce alloys was discovered experimentally (see Refs. 19–21). The magnetic phase diagram of $CeNi_{1-x}Cu_x$ exhibits change of magnetic ordering from AFM to ferromagnetic (FM) at $x=0.8$, whereas for $0.2 < x < 0.8$ the SG state appears only at high temperatures above the FM order. Apparently, the Kondo interaction could be considered as the mechanism leading to the reduction of magnetic moments because increasing Ni contents effectively reduces the strength of the indirect exchange interaction, and then, a larger temperature stability range of the SG phase appears (see Refs. 19 and 20).

The competition between the one-site Kondo-type correlations and the indirect intersite exchange is visualized in Doniach's diagram where possible phase transition and crossover energies are plotted as functions of a "bare" coupling parameter $\alpha = J/\varepsilon_F$ characterizing the exchange interaction between the spin and electron subsystems in KL's.²² Only Kondo screening and RKKY coupling were competing in the original Doniach diagram. Later on it was noticed that the trend to spin liquid (SL) ordering is the third type of correlation which modifies essentially the magnetic phase diagram of KL's in a critical region $T_K \sim I$ of the Doniach diagram.^{23–25}

In this paper we present a high-temperature mean-field description of transitions from a paramagnetic state to correlated spin states in KL's, which does not violate the local constraint for the spin-fermion operators. We use the Popov-Fedotov representation of spin operators²⁶ to construct the effective action for KL's. In this representation the local constraint is rigorously fulfilled. We consider the mutual influence of various order parameters (Kondo, AFM, SL, and SG correlation functions) and derive a Ginzburg-Landau functional (Sec. II). On the basis of this functional we construct generalized Doniach's diagrams that take into account all the

interplays. The Doniach diagram for a perfect KL is presented in Sec. III and the influence of Kondo screening on the SG diagram for a disordered KL is considered in Sec. IV.

All existing theories appeal to mean-field approximations that violate the local gauge invariance both in the Kondo and SL channels.²⁷ As a result, fictitious second-order phase transitions from a free spin (paramagnetic) state to a confined spin (Kondo singlet or resonating valence bond SL) state arise in spite of the fact that neither symmetry is violated by these transformations. A different approach allows us to get rid of the assumption of a Kondo-type ‘‘condensate’’ within the framework of a mean-field theory. To eliminate the fictitious phase transition to a SL state one should refrain from a mean-field approach to the SL mode. We offer a scenario of a continuous crossover from a paramagnetic state of localized spins to the SL state, where the interplay between critical AFM fluctuations and Kondo screening clouds in KL’s results in ‘‘Fermionization’’ of spin excitations at low temperatures (Sec. V). In Sec. VI the interrelations between the theory and real heavy fermion systems is briefly discussed.

II. DERIVATION OF EFFECTIVE ACTION

The Hamiltonian of the KL model is given by

$$H = \sum_{k\sigma} \varepsilon_k c_{k\sigma}^\dagger c_{k\sigma} + J \sum_j \left(\mathbf{S}_j \mathbf{s}_j + \frac{1}{4} N_j n_j \right). \quad (1)$$

Here the local electron and spin-density operators for conduction electrons at site j are defined as

$$n_j = \sum_{j\sigma} c_{j\sigma}^\dagger c_{j\sigma}, \quad \mathbf{s}_j = \sum_{\sigma\sigma'} \frac{1}{2} c_{j\sigma}^\dagger \hat{\tau}_{\sigma\sigma'} c_{j\sigma'}, \quad (2)$$

where $\hat{\tau}$ are the Pauli matrices and $c_{j\sigma} = \sum_k c_{k\sigma} \exp(ikj)$. The SG freezing is possible if an additional quenched randomness of the intersite exchange I_{jl} between the localized spins arises. This disorder is described by

$$H' = \sum_{jl} I_{jl} (\mathbf{S}_j \mathbf{S}_l). \quad (3)$$

We start with a perfect Kondo lattice. The spin correlations in KL’s are characterized by two energy scales, i.e., $I \sim J^2/\varepsilon_F$, and $\Delta_K \sim \varepsilon_F \exp(-\varepsilon_F/J)$ (the intersite indirect exchange of the Ruderman-Kittel-Kasuya-Yosida (RKKY) type and the Kondo binding energy, respectively). At high enough temperatures the localized spins are weakly coupled with the electron Fermi sea having the Fermi energy ε_F , so that the magnetic response of a rare-earth sublattice of a KL is of paramagnetic Curie-Weiss type. With decreasing temperature either a crossover to a strong-coupling Kondo singlet regime occurs at $T \sim \Delta_K$ or the phase transition to an AFM state occurs at $T = T_N \sim zI$ where z is a coordination number in the KL. If $T_N \approx \Delta_K$ the interference between two trends results in the decrease of both characteristic temperatures or in suppressing one of them. As was noticed in Refs. 24 and 28, in this case the SL correlations with characteristic energies $\Delta_s \sim I$ may overcome the AFM correlations, and the spin subsystem of the KL can condense in a SL state yet in a region of weak Kondo coupling.

To describe all three modes in a unified way one should derive a free-energy functional $\mathcal{F}(T)$ in a region of $T > (T_N, \Delta_K, \Delta_s)$. First, we integrate out the highest energies $\sim \varepsilon_F$. Here and below we use the dimensionless coupling constants $J \rightarrow J/\varepsilon_F$, $I \rightarrow I/\varepsilon_F$, etc. Since we are still in a weak-coupling limit of Kondo-type scattering, we may restrict ourselves to the standard high-temperature renormalization of the one site coupling $J \rightarrow \tilde{J}(T) = 1/\ln(T/\Delta_K)$ and the second-order equation of perturbation theory in J for RKKY interaction. As a result, one arrives at an effective Hamiltonian

$$\begin{aligned} \tilde{H} = & \sum_{k\sigma} \varepsilon_k c_{k\sigma}^\dagger c_{k\sigma} + \tilde{J} \sum_j \mathbf{s}_j \mathbf{S}_j - I \sum_{jl} \mathbf{S}_j \mathbf{S}_l \\ & + gh \sum_j (-1)^j S_j^z. \end{aligned} \quad (4)$$

Here all energies are measured in $\varepsilon_F = 1$ units, and an infinitesimal staggered magnetic field is introduced that respects the symmetry of the magnetic bipartite lattice in the AFM case (ε_F is restored in further calculations wherever it is necessary).

To calculate the spin part of the free energy $\mathcal{F}_s(T) = -T \ln \mathcal{Z}_s$ we represent the partition function \mathcal{Z} in terms of a path integral. The spin subsystem is described by means of the Popov-Fedotov trick²⁶

$$\mathcal{Z}_s = \text{Tr} e^{-\beta H} = i^N \text{Tr} e^{-\beta [H + i\pi N^f / (2\beta)]}. \quad (5)$$

Here $\beta = T^{-1}$, N is the number of unit cells, $N^f = \sum_j N_j^f$, and the spin $S = 1/2$ operators are represented by bilinear combinations of fermion operators

$$S_j^z = (f_{j\uparrow}^\dagger f_{j\uparrow} - f_{j\downarrow}^\dagger f_{j\downarrow})/2, \quad S_j^+ = f_{j\uparrow}^\dagger f_{j\downarrow}, \quad S_j^- = f_{j\downarrow}^\dagger f_{j\uparrow}. \quad (6)$$

These operators obey the constraint

$$N_j^f = \sum_{\sigma} f_{j\sigma}^\dagger f_{j\sigma} = 1. \quad (7)$$

In accordance with Ref. 26, the Lagrange term with a fixed imaginary chemical potential $-i\pi T/2$ is added to the Hamiltonian (1). We use the path-integral representation for the partition function,

$$\frac{\mathcal{Z}}{\mathcal{Z}^0} = \frac{\int D\bar{c} Dc D\bar{f} Df \exp \mathcal{A}}{\int D\bar{c} Dc D\bar{f} Df \exp \mathcal{A}_0}. \quad (8)$$

Then the Euclidean action for the KL is given by

$$\begin{aligned} \mathcal{A} = & \mathcal{A}_0 - \int_0^\beta d\tau \mathcal{H}_{int}(\tau), \\ \mathcal{A}_0 = & \mathcal{A}_0[c, f] = \int_0^\beta d\tau \sum_{j\sigma} \{ \bar{c}_{j\sigma}(\tau) [\partial_\tau - \varepsilon(-i\nabla) + \mu] c_{j\sigma}(\tau) \\ & + \bar{f}_{j\sigma}(\tau) (\partial_\tau - i\pi T/2) f_{j\sigma}(\tau) \}. \end{aligned} \quad (9)$$

Following the Popov-Fedotov procedure, the imaginary chemical potential is included in discrete Matsubara frequencies for semifermission operators $f_{j\sigma}$. As a result the Matsubara frequencies are determined as $\omega_m = 2\pi T(m + 1/4)$ for spin semifermissions and $\epsilon_n = 2\pi T(n + 1/2)$ for conduction electrons. In terms of the temperature Green's function the Euclidian action has the form

$$\begin{aligned} \mathcal{A} = & \mathcal{A}_0 + \mathcal{A}_{int} = \sum_{k\sigma} \bar{c}_{k\sigma} G_0^{-1}(k) c_{k\sigma} \\ & + \sum_{j\sigma} \bar{f}_{j\sigma}(\omega_n) D_{0\sigma}^{-1}(\omega_n) f_{j\sigma}(\omega_n) \\ & + \frac{\bar{J}}{2} \sum_{j\sigma\sigma'} \sum_{\epsilon_m, \omega_n} \bar{c}_{j\sigma}(\epsilon_1) f_{j\sigma}(\omega_2) \bar{f}_{j,\sigma'}(\omega_1) c_{j,\sigma'}(\epsilon_2) \\ & \times \delta_{\epsilon_1 - \epsilon_2, \omega_1 - \omega_2} + I \sum_{j\ell, \sigma\gamma} \sum_{\omega_n} \bar{f}_{j\sigma}(\omega_1) \\ & \times \hat{\tau}_{\sigma\sigma'} f_{j,\sigma'}(\omega_2) \bar{f}_{\ell, \gamma}(\omega_3) \hat{\tau}_{\gamma\gamma'} f_{\ell, \gamma'}(\omega_4) \delta_{\omega_1 - \omega_2, \omega_3 - \omega_4}. \end{aligned} \quad (10)$$

Here the Green's functions (GF's) for bare quasiparticles are

$$G_0(k, i\epsilon_n) = \frac{1}{i\epsilon_n - \epsilon_k + \mu}, D_{0\sigma}^\nu(i\omega_m) = \frac{1}{i\omega_m - \sigma g h^\nu / 2} \quad (11)$$

(ν is the index of magnetic sublattice that defines the direction of the staggered magnetic field).

The first interaction term in this equation is responsible for *low-energy* Kondo correlations, and we will treat it in conventional manner.²⁹ In the RKKY term two modes should be considered, namely the local mode of AFM fluctuations^{30,31} and the nonlocal spin liquid correlations.^{31,32} For these modes we adopt the Néel-type antiferromagnetism and the resonating valence bond (RVB) type spin liquid state, respectively. In accordance with the general path-integral approach to KL's, we first integrate over fast (electron) degrees of freedom. Then in the *sf*-exchange contribution to the action (10) we are left with the auxiliary field ϕ with a statis-

tics complementary to that of semifermissions.³³ The spin correlations in the intersite RKKY term are treated in terms of vector Bose fields \mathbf{Y} (AFM mode) and a scalar field W (spin liquid RVB mode). As a result, \mathcal{A}_{int} is represented by the following expression:

$$\begin{aligned} \mathcal{A}_{int} = & -\frac{2}{\bar{J}} \text{Tr} |\phi|^2 - \text{Tr} \frac{1}{I_{\mathbf{q}}} \mathbf{Y}_{\mathbf{q}} \mathbf{Y}_{-\mathbf{q}} - \text{Tr} \frac{1}{I_{\mathbf{q}_1 - \mathbf{q}_2}} W_{\mathbf{P}\mathbf{q}_1} W_{\mathbf{P}\mathbf{q}_2} \\ & - \text{Tr} \bar{f}_{j\sigma} \phi_j G_0(\mathbf{r}) \bar{\phi}_l f_{l\sigma}. \end{aligned} \quad (12)$$

When making a Fourier transformation for nonlocal spin liquid correlations (the third term on the right hand side) we introduced the coordinates $\mathbf{R} = (\mathbf{R}_j + \mathbf{R}_l)/2$ and $\mathbf{r} = \mathbf{R}_j - \mathbf{R}_l$ for the RVB field, and \mathbf{P}, \mathbf{q} are the corresponding momenta. Below we assume $\mathbf{P} = 0$ and omit it in notations for the SL mode, $W_{0\mathbf{q}} \equiv W_{\mathbf{q}}$.

A consequent mean-field approach demands the introduction of three "condensates," i.e., three time-independent *c*-fields for Kondo coupling, AFM coupling, and SL coupling, respectively, that arise as a consequence of a saddle-point approximation for all three modes. For example, the mean-field description of the interplay between the Kondo and RVB couplings was presented in Refs. 23 and 25. The undesirable consequence of this approximation is the violation of the electromagnetic U(1) gauge invariance, when the electrical charge is ascribed to an initially neutral spin fermion field f (see, e.g., Ref. 12). According to a scenario offered in Refs.²⁴ and 32, there is no necessity of introducing the mean-field saddle point for Kondo coupling because the transition to a correlated spin state occurs at $T > T_K$. In this case the one site Kondo correlations suppress the Néel phase transition (reduce $T_N^0 \rightarrow T_N$) in favor of the spin liquid state with a characteristic crossover temperature $T^* > T_N$. Therefore we refrain from using the saddle-point approximation for the field ϕ but still use it for the fields \mathbf{Y} and W .

To condense the equation for the action \mathcal{A} we introduce a spinor representation for semifermissions

$$\bar{F}_{\mathbf{p}} = (\bar{f}_{\mathbf{p}\uparrow} \bar{f}_{\mathbf{p}\downarrow} \bar{f}_{\mathbf{p}+\mathbf{Q}\uparrow} \bar{f}_{\mathbf{p}+\mathbf{Q}\downarrow}),$$

and the following definition of the Fourier transform of the inverse semi-fermionic Green's function

$$D_m^{-1}(W_{\mathbf{p}}, \mathbf{Y}_{\mathbf{Q}}) = \begin{pmatrix} i\omega_m - W_{\mathbf{p}} & 0 & Y_{\mathbf{Q}}^z & Y_{\mathbf{Q}}^+ \\ 0 & i\omega_m - W_{\mathbf{p}} & Y_{\mathbf{Q}}^- & -Y_{\mathbf{Q}}^z \\ Y_{\mathbf{Q}}^z & Y_{\mathbf{Q}}^+ & i\omega_m - W_{\mathbf{p}+\mathbf{Q}} & 0 \\ Y_{\mathbf{Q}}^- & -Y_{\mathbf{Q}}^z & 0 & i\omega_m - W_{\mathbf{p}+\mathbf{Q}} \end{pmatrix}. \quad (13)$$

The same function in a lattice representation is presented in Appendix A. This operator arises as a result of the Hubbard-Stratonovich transformation decoupling the magnetic modes \mathbf{Y} and the spin-liquid mode W . Then the effective action \mathcal{A}_s acquires the form

$$\mathcal{A}_s = \text{Tr} \bar{F} D_m^{-1} F + \mathcal{A}_{int}. \quad (14)$$

Now we integrate over semi-Fermionic fields and obtain the effective action for a KL model,

$$\begin{aligned} \mathcal{A}_s = & \text{Tr} \ln [D_m^{-1}(\mathbf{Y}, W) + \phi_j G_0(\mathbf{r}) \bar{\phi}_l] - \frac{2}{j} \text{Tr} |\phi|^2 \\ & - \text{Tr} \frac{1}{I_{\mathbf{q}}} \mathbf{Y}_{\mathbf{q}} \mathbf{Y}_{-\mathbf{q}} - \text{Tr} \frac{1}{I_{\mathbf{q}_1 - \mathbf{q}_2}} W_{\mathbf{q}_1} W_{\mathbf{q}_2}. \end{aligned} \quad (15)$$

Here the argument $|\phi|^2$ appears in the Green's function D_m as a result of integration of the last term in Eq. (12) over the semi-Fermionic fields.

In a mean-field approximation for two independent modes (neglecting renormalization due to Kondo scattering) Eq. (15) results in a free energy with two local minima reflecting two possible instabilities of the high-temperature paramagnetic state relative to the Néel and SL states. To describe these instabilities one should pick out the classic part of the Néel field,

$$\mathbf{Y} = (\beta N)^{1/2} \frac{I_{\mathbf{q}}}{2} \mathcal{N} \delta_{\mathbf{q}, \mathbf{Q}} \delta_{\omega, 0} \mathbf{e}_z + \tilde{\mathbf{Y}}_{\mathbf{q}}, \quad (16)$$

and use the eikonal approximation for the SL field,

$$W_{\mathbf{R}, \mathbf{r}} = I \Delta(\mathbf{r}) \exp(i\theta). \quad (17)$$

Here $\mathcal{N} = \langle Y_{\mathbf{Q}}^z \rangle$ is the staggered magnetization, $\tilde{\mathbf{Y}}_{\mathbf{q}}$ are the fluctuations around the mean-field magnetization, \mathbf{Q} is the AFM vector for a given bipartite lattice, \mathbf{e}_z is the unit vector along the magnetization axis, $\Delta(\mathbf{r})$ is the modulus of RVB field, and $\theta = [\mathbf{r} \cdot \mathbf{A}(\mathbf{R})]$ is the phase of this field.

It is known for Heisenberg lattices dimensions $d > 1$ that T_N is higher than the temperature T_{sl} of the crossover to the SL state, so that the ordered magnetic phase is the Neel phase. Due to Kondo fluctuations that screen dynamically local magnetic correlations and slightly enhance the intersite semi-Fermionic correlations, the balance between two modes is shifted towards the spin liquid phase in a critical region of Doniach's diagram, $T_K \sim I$. To show this we include in the free energy the corresponding corrections induced by the last term in Eq. (12). As was mentioned above we refrain from using the mean-field approach to the Kondo field, so that the interplay between the Kondo mode and two other modes is taken into account by including the Néel mean-field corrections to the semi-Fermionic Green's function. Then instead of Eq. (13) one has the following equation for D^{-1} :

$$\begin{aligned} & D_m^{-1}(\mathcal{N}, \Delta) \\ & = \begin{pmatrix} i\omega_m - \Delta I_{\mathbf{q}} & 0 & \mathcal{N} I_{\mathbf{Q}}/2 & 0 \\ 0 & i\omega_m - \Delta I_{\mathbf{q}} & 0 & -\mathcal{N} I_{\mathbf{Q}}/2 \\ \mathcal{N} I_{\mathbf{Q}}/2 & 0 & i\omega_m - \Delta I_{\mathbf{q}} & 0 \\ 0 & -\mathcal{N} I_{\mathbf{Q}}/2 & 0 & i\omega_m - \Delta I_{\mathbf{q}} \end{pmatrix}. \end{aligned} \quad (18)$$

The next steps, i.e., calculation of fluctuation corrections to the stationary point mean-field solutions, can be performed by introducing the auxiliary self-energies,

$$M(\tilde{\mathbf{Y}}, \theta) = D_m^{-1}(\mathbf{Y}, W) - D_m^{-1}(\mathcal{N}, \Delta)$$

$$K_{\phi}(\omega_{n_1}, \omega_{n_2}) = -T \sum_{\Omega} \phi_j(\omega_{n_1} - \Omega) G_0(\mathbf{r}, \Omega) \bar{\phi}_l(\omega_{n_2} - \Omega). \quad (19)$$

Then the effective action is approximated by the polynomial expansion

$$\begin{aligned} \text{Tr} \ln [D_m^{-1}(\mathbf{Y}, W) + K_{\phi}] &= \text{Tr} \ln D_m^{-1}(\mathcal{N}, \Delta) \\ &+ \text{Tr} \sum_{n=1}^{\infty} \frac{(-1)^{n+1}}{n} \{D_m(\mathcal{N}, \Delta) \\ &\times [M(\tilde{\mathbf{Y}}, \theta) + K_{\phi}]\}^n \end{aligned} \quad (20)$$

(the Fourier transform of the diagonal part of the Green's function K_{ϕ} is calculated in Appendix A).

Neglecting all fluctuations, i.e., retaining only the first term in the right hand side of Eq. (20) together with quadratic terms for the AFM and SL modes (15), one obtains the following expression for the free energy per lattice cell:

$$\begin{aligned} \beta \mathcal{F}(\mathcal{N}, \Delta) &= \frac{\beta z |I| \mathcal{N}^2}{4} - \ln [2 \cosh(\beta z I \mathcal{N} / 2)] \\ &+ \frac{\beta z |I| \Delta^2}{2} - \sum_{\mathbf{q}} \ln [2 \cosh(\beta I_{\mathbf{q}} \Delta)] \end{aligned} \quad (21)$$

($I_{\mathbf{Q}} = -I$). The standard self-consistent mean-field equations for the order parameters are obtained from the condition of minima of the free energy. These are

$$\mathcal{N} = \tanh\left(\frac{I_{\mathbf{Q}} \mathcal{N}}{2T}\right) \quad (22)$$

for the Néel parameter and

$$\Delta = - \sum_{\mathbf{q}} \nu(\mathbf{q}) \tanh\left(\frac{I_{\mathbf{q}} \Delta}{T}\right) \quad (23)$$

for the real part of the RVB order parameter. Here $\nu(\mathbf{q}) = I_{\mathbf{q}} / I_0$. The latter equation was first derived in Ref. 34.

Then making the high-temperature expansion of Eq. (21), one obtains a Ginzburg-Landau (GL) equation in the approximation of two independent modes:

$$\beta \mathcal{F}(\mathcal{N}, \Delta) = \frac{\beta |I| z \mathcal{N}^2}{4} \tau_N + c_N \mathcal{N}^4 + \frac{\beta |I| z \Delta^2}{2} \tau_{sl} + c_{sl} \Delta^4 \quad (24)$$

where $\tau_N = 1 - T_N/T$ and $\tau_{sl} = 1 - T_{sl}/T$. The temperatures of two magnetic instabilities are determined as the temperatures of sign inversion in the coefficients in the quadratic terms of the GL expansion $T_N = z|I|/2$ and $T_{sl} = |I|$. The fourth-order GL coefficients c_N and c_{sl} are positive and depend only on temperature. Up to this point the theory is formulated for arbitrary dimension d . In fact, the dimensionality enters the RKKY coupling parameter (see below) and determines the number of nearest neighbors z . We consider zI as a universal parameter in further calculations.

III. DONIACH'S DIAGRAM REVISITED

To describe the contribution of Kondo scattering to the magnetic part of the Doniach's diagram one should integrate \mathcal{A} over the auxiliary field ϕ and thus find the Kondo corrections to both the Néel and RVB instability points. One should

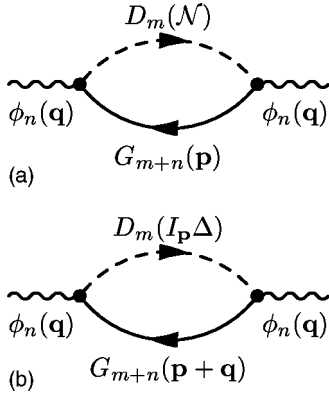


FIG. 1. Diagrams for the fluctuation contribution to the effective action responsible for Kondo screening corrections to magnetic (a) and spin liquid (b) correlations.

consider two cases: (i) $T_N > T_{sl}$ (Kondo corrections screen AFM magnetic moments), and (ii) $T_{sl} > T_N$ (Kondo corrections enhance nonlocal RVB correlations).

(i) *Kondo screening of AFM order.* In this case one takes $\Delta = 0$ in the Green's function (18). Then adding the last term of Eq. (12) to the effective action and integrating over the semi-Fermionic fields yields the correction to the effective action in a form of polarization operators given by the first diagram in Fig. 1(a).

Here the external wavy lines stand for the “semi-Bosonic” field ϕ describing Kondo correlations (see Ref. 33). These semi-Bosonic fields are still bosons from the point of view of the permutation relations, but unlike true Bosonic fields they do not satisfy symmetric boundary conditions, and cannot condense in a state with zero frequency and momentum. So the Popov-Fedotov formalism gives an adequate description of the fact that there is no broken symmetry corresponding to the Kondo temperature.³⁵ The polarization loop is formed by the conduction electron propagator G_0 (solid line) and local semi-Fermionic Green's function D_m given by Eq. (18) (see Appendix A for the explicit form of these Green's functions). As a result the modified effective action is

$$\mathcal{A}_\phi = 2 \sum_{\mathbf{q}, n} \left[\frac{1}{\tilde{J}} - \delta\Pi(\mathcal{N}) \right] |\phi_n(\mathbf{q})|^2. \quad (25)$$

The logarithmic renormalization of the coupling constant is already taken into account in \tilde{J} . Therefore the dimensionless integral $\delta\Pi$ includes only contributions due to a nonzero magnetic molecular field,³⁶

$$\delta\Pi(\mathcal{N}) = \left[\frac{\pi}{2} \left(\frac{1}{\cosh(\beta\mathcal{N})} - 1 \right) + O\left(\frac{\mathcal{N}^2}{T\epsilon_F}\right) \right]. \quad (26)$$

(see Appendix B for detailed calculations). This correlation correction should be incorporated in the equation for the free energy, so that

$$\beta\mathcal{F}(\mathcal{N}) = \beta\mathcal{F}(\mathcal{N}, 0) + \text{Tr} \ln \left[\frac{1}{\tilde{J}} - \delta\Pi(\mathcal{N}) \right]. \quad (27)$$

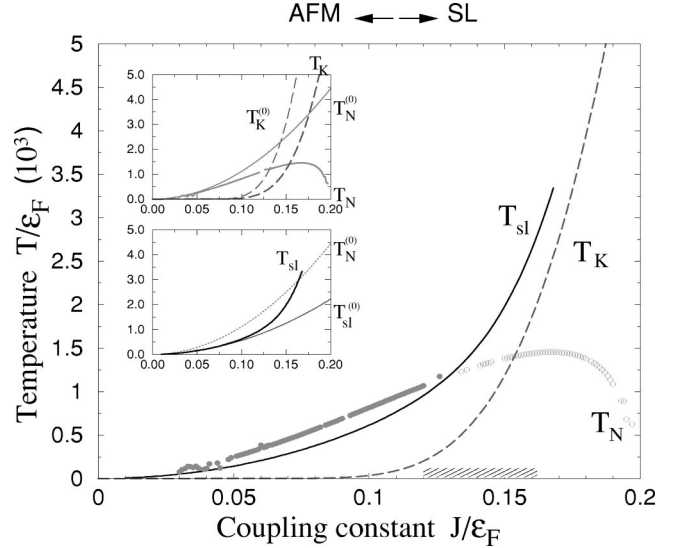


FIG. 2. Doniach's diagram with modifications due to Kondo screening (see text for explanation).

Then differentiation of Eq. (27) with respect to the Néel order parameter \mathcal{N} gives the following self-consistent equation in the vicinity of the renormalized transition point,

$$\mathcal{N} = \tanh \left(\frac{I_Q \mathcal{N}}{2T} \right) \left[1 - \frac{a_N}{\ln(T/T_K)} \frac{\cosh^2(\beta I_Q \mathcal{N}/2)}{\cosh^2(\beta I_Q \mathcal{N})} \right] \quad (28)$$

instead of Eq. (22). Here the Kondo temperature T_K is defined as the temperature where the coefficient in front of $|\phi_{n=0}|^2$ in Eq. (25), i.e., the function $\tilde{J}^{-1} - \delta\Pi(\mathcal{N})$, turns to zero. It is seen that the screening corrections near the Néel transition point are negative, $\delta\Pi(\mathcal{N} \rightarrow 0) = -a_N(\beta\mathcal{N})^2 < 0$, so that Kondo screening effectively increases the magnetic free energy, and eventually the logarithmic local-field corrections *reduce* the Néel temperature. The numerical solution of Eq. (28) is shown by the circles in Fig. 2. The top inset illustrates the reduction of T_N in comparison with the bare mean-field Néel temperature $T_N^0 = z\epsilon_F \alpha^2/2$, where $\alpha = J/\epsilon_F$ is the dimensionless coupling constant for the Doniach's diagram.

(ii) *Kondo enhancement of SL transition.* Now we assume $\mathcal{N} = 0$ in Eq. (21) and subsequent equations. Following the same lines as in the preceding subsection, one obtains the modified effective action

$$\mathcal{A}_\phi = 2 \sum_{\mathbf{q}, n} \left[\frac{1}{\tilde{J}} - \delta\Pi(I_q \Delta) \right] |\phi_n(\mathbf{q})|^2 \quad (29)$$

instead of Eq. (25), and the polarization integral with the use of the diagram (b) from Fig. 1 is given by

$$\delta\Pi(I_q \Delta) = \sum_{\mathbf{k}} \left[\frac{1}{\cosh \beta(I_k \Delta)} - 1 + I_k \Delta \tanh(\beta I_k \Delta) \right] \times \frac{1}{\xi_{\mathbf{k}+\mathbf{q}}^2 + (\pi/2\beta)^2}, \quad (30)$$

instead of Eq. (26) (see Appendix B). Here $\xi_{\mathbf{p}} = \varepsilon_{\mathbf{p}} - \varepsilon_F$ is the dispersion law for conduction electrons near the Fermi surface. Inserting the corresponding corrections to the free energy,

$$\beta\mathcal{F}(\Delta) = \beta\mathcal{F}(0, \Delta) + \text{Tr} \ln \left[\frac{1}{\mathcal{J}} - \delta\Pi(I_{\mathbf{q}}\Delta) \right]. \quad (31)$$

one obtains the corrected self-consistent equation for Δ . When deriving this equation, the spinon dispersion can be neglected since $\Delta \rightarrow 0$ in a critical point. Then one has

$$\Delta = - \sum_{\mathbf{q}} \nu(\mathbf{q}) \left[\tanh\left(\frac{I(\mathbf{q})\Delta}{T}\right) + a_{sl} \frac{I_{\mathbf{q}}\Delta}{T \ln(T/T_K)} \right]. \quad (32)$$

Here $a_{sl} \sim 1$ is a numerical coefficient. It is seen from Eq. (32) that unlike the case of local magnetic order, Kondo scattering favors transition to the SL state, because this scattering means in fact involvement of itinerant electron spin degrees of freedom into spinon dynamics. Mathematically, enhancement arises because $\delta\Pi(I_{\mathbf{q}}\Delta \rightarrow 0) = a_{sl}(\beta I_{\mathbf{q}}\Delta)^2 > 0$, so that Kondo ‘‘antiscreening’’ effectively decreases the magnetic free energy. The results of the numerical solution of Eqs. (31) and (32) are represented by circles in Fig. 2.

Here filled circles correspond to the region where the AFM order overcomes the SL phase, and the light circles show unphysical ‘‘suppressed’’ AFM solutions obtained beyond the region of validity of the mean-field equation (28). Two other characteristic temperatures, renormalized T_K and T_{sl} , are shown by dashed and solid lines, respectively. The effects of suppression of T_N (thin and thick solid lines for bare and renormalized temperatures) and T_K (thin and thick dotted lines) are illustrated by the upper and lower inset, respectively. As is seen from the modified Doniach’s diagram, the interplay between three modes becomes significant in a critical region where the exchange coupling constant is close to the point $\alpha_c = 0.13$ where $I = \Delta_K$ in the conventional Doniach’s diagram. If the Kondo screening is not taken into account, then $T_{sl}^{(0)}(\alpha) < T_N^{(0)}(\alpha)$ (thin solid and dotted lines in the lower inset). The Kondo screening changes this picture radically, and as a result, a wide enough interval of the parameter α just to the right of the critical value α_c arises, where the enhanced transition temperature T_{sl} exceeds both the reduced Néel temperature T_N and the Kondo temperature T_K . The calculations of T_{sl} presented in Fig. 2 are performed for $d=2$. A similar picture exists for $d=3$, although the domain of the stable SL state is more narrow (for a given value of zI). This means that in this region the stable magnetic phase is, in fact, the spin liquid phase. If one descends from high temperatures in a hatched region of Doniach’s diagram where $T_K \sim T_N$, the Kondo scattering suppresses the AFM correlations, but the SL correlations quench the Kondo processes at some temperature $T_{sl} > T_K$. As a result the Kondo-type saddle point is not realized in the free-energy functional in agreement with the assumption made above in our derivation of Ginzburg-Landau expansion. The preliminary version of this scenario was presented in Ref. 24. The more refined mean-field approach described here confirms and enhances this scenario, however, the SL liquid phase is

still described in the mean-field approximation. Although the local constraint for spin operators is not violated in the Popov-Fedotov formalism, the gauge phase is still fixed,²⁷ so the next task is the consideration of fluctuation back flows described by the higher-order terms of the Ginzburg-Landau expansion.

IV. ISING SPIN GLASSES IN DONIACH’S DIAGRAM

In this section we consider the interplay between Kondo scattering and magnetic correlations in the case of a *random* RKKY interaction (3), where the randomness results in the formation of a spin-glass phase. We consider disorder induced by paramagnetic impurities in KL. As was shown in Ref. 37, elastic scattering results in the appearance of a random phase $\delta(r)$ in RKKY indirect exchange parameter,

$$I_{ij} \equiv I(r) \simeq - \left(\frac{J^2}{\varepsilon_F} \right) \frac{\cos \left[2p_F r - \frac{\pi}{2}(d+1) + \delta(r) \right]}{(2p_F r)^d}, \quad (33)$$

where $r = |R_i - R_j|$ and d is the dimensionality of the KL. This form of random exchange predetermines two possible scenarios of SG ordering.

(i) Fluctuations take place around a node of the RKKY interaction (33). This asymptotic behavior is derived from the general equation for the RKKY exchange parameter,^{38,39}

$$I_{ij} = - \frac{J^2}{\varepsilon_F} \frac{\pi}{d-1} \left(\frac{p_F a_0^2}{2\pi r} \right)^d (p_F r)^2 [J_{d/2-1}(p_F r) Y_{d/2-1}(p_F r) + J_{d/2}(p_F r) Y_{d/2}(p_F r)].$$

[a_0 is the lattice spacing, $J_\nu(x)$ and $Y_\nu(x)$ are the Bessel functions of the first and second kind]. In this case FM and AFM bonds enter the partition function on equal footing, and quenched independent random variables I_{ij} can be described by a Gaussian distribution $P(I_{ij}) \sim \exp[-I_{ij}^2 N / (2I^2)]$.⁴⁰ The magnetic ordering effects also can be included in our approach by introducing a nonzero standard deviation $\Delta I \neq 0$ into the distribution $P(I_{ij})$ that, in turn, results in additional competition between SG and AFM (or, in some cases, FM) states. Recently, the competition between AFM and SG regimes was considered in Ref. 41.

(ii) RKKY exchange fluctuates around some negative value in the AFM domain of exchange parameters. In this case there is a competition between SG, SL, and AFM phases. The third possibility, i.e., fluctuations in the FM domain is somewhat trivial because in this case Kondo fluctuations cannot significantly change the freezing scenario.

We start with the case (i). To understand the situation qualitatively we make the following simplifying approximations. First, we consider only a Ising-like exchange in the Hamiltonian (3):

$$H' = - \sum_{\langle ij \rangle} I_{ij} S_i^z S_j^z. \quad (34)$$

This is a usual approximation in the theory of spin glasses that allows one to forget about the quantum dynamics of the

spin variables.⁴² In the original paper⁴³ the simplifying assumptions ($d=\infty$, separate electron bath for each localized spin) were made. Thus the form of the spin-spin correlator was predetermined, and these assumptions allowed the authors to obtain an exact solution in a framework of dynamical mean-field theory. We refrain from using these approximations. Second, we confine ourselves with the mean-field (replica symmetric) solution of the Edward-Anderson (EA) model.⁴⁴ This means that only a pairwise interaction of nearest neighbors is taken into account. The number z of nearest neighbors should be big enough ($z^{-1}\ll 1$) to justify the mean-field approximation. We consider the interplay between SG and Kondo-type correlations by means of the replica method. We use the approach developed in Ref. 45 for the Sherrington-Kirkpatrick model.⁴⁶ Both electron and semiferion variables are replicated ($c\rightarrow c^a, f\rightarrow f^a$, where $a=1, \dots, n$), and the number of replicas is tended to zero, so that the free energy per cell is given by the limit $\mathcal{F}=\beta^{-1}\lim_{n\rightarrow 0}(1-\langle Z^n \rangle_{av})/(nN)$. Here the replicated partition function is

$$\langle Z^n \rangle_{av} = \prod \int dI_{ij} P(I_{ij}) \prod D\{c_{i,\sigma}^a, f_{i,\sigma}^a\} \times \exp\left(\mathcal{A}_0[c^a, f^a] - \int_0^\beta d\tau H_{int}(\tau)\right) \quad (35)$$

where \mathcal{A}_0 (10) corresponds to noninteracting fermions.

Averaging over disorder and integrating out high-energy electronic states by virtue of a replica-dependent Hubbard-Stratonovich transformation one arrives at the following equation

$$\langle Z^n \rangle_{av} = \prod \int D\{c^a, f^a, \phi^a\} \exp\left(\mathcal{A}_0 + \frac{zI^2}{4N} \text{Tr}[X^2] + \int_0^\beta d\tau \text{Tr}\left\{\phi^a \bar{c}^a f^a + \bar{\phi}^a \bar{f}^a c^a - \frac{2}{J} |\phi^a|^2\right\}\right) \quad (36)$$

with

$$X^{ab}(\tau, \tau') = \sum_i \sum_{\sigma, \sigma'} \bar{f}_{i,\sigma}^a(\tau) \sigma f_{i,\sigma}^a(\tau) \bar{f}_{i,\sigma'}^b(\tau') \sigma' f_{i,\sigma'}^b(\tau').$$

Then following the standard pattern of replica theory for spin glasses^{45,47} one fixes the saddle point in spin space related to the EA order parameter q_{EA} . At this stage the initial problem is mapped onto a set of independent Kondo scatterers for low energy conduction electrons in external replica dependent effective magnetic field:

$$\langle Z^n \rangle_{av} = \exp\left(-\frac{1}{4} z(\beta I)^2 N [n\bar{q}^2 + n(n-1)q^2] + \sum_i \ln \left[\prod \int D\{f^a, \phi^a\} \int_x^G \int_{y^a}^G \times \exp(\mathcal{A}\{f^a, \phi^a, y^a, x\}) \right] \right) \quad (37)$$

where $\int_x^G f(x)$ denotes $\int_{-\infty}^\infty dx / \sqrt{2\pi} \exp(-x^2/2) f(x)$,

$$\mathcal{A}\{f^a, \psi^a, y^a, x\} = \sum_{a,\sigma} \bar{f}_\sigma^a [(D_m^{(a)})^{-1} - \sigma h(y^a, x)] f_\sigma^a - \frac{2}{J} \sum_n |\phi_n^a|^2 \quad (38)$$

and $h(y^a, x) = I\sqrt{zqx} + I\sqrt{z(\bar{q}-q)}y^a$ is an effective local magnetic field, which depends on the diagonal and off-diagonal elements of the Parisi matrix, $\bar{q} = \langle S_i^a(0) S_i^a(t \rightarrow \infty) \rangle$ and $q = \langle S_i^a(0) S_i^b(t \rightarrow \infty) \rangle$ ($a \neq b$), respectively. The latter one is the EA order parameter $q_{EA} = q$. Neglecting all fluctuations and retaining only the first two terms in the exponent in Eq. (37), one comes to the EA mean-field equation for the free energy,

$$\beta\mathcal{F} = \frac{z(\beta I)^2}{4} [(1-\bar{q})^2 - (1-q)^2] - \int_x^G \ln[2 \cosh(\beta I x \sqrt{zq})]. \quad (39)$$

(see Ref. 47). Then making the high-temperature expansion, one obtains the Ginzburg-Landau equation in the vicinity of the SG transition,⁴⁸

$$\beta\mathcal{F}_{sg} = \frac{z(\beta I)^2}{4} q^2 \tau_{sg} - c_{sg} q^3 + d_{sg} q^4, \quad (40)$$

where $\tau_{sg} = 1 - T_f/T$ and $T_f = \sqrt{z}I$ is a spin-glass freezing temperature.

Like in the previous case of the ordered KL we incorporate the static replica dependent magnetic field h in semi-Fermionic Green's functions. As a result, the modified effective action for the Kondo fields arises like in Eqs. (25) and (29),

$$\mathcal{A}[y^a, x] = \ln\{2 \cosh[\beta h(y^a, x)]\} - \sum_n \left[\frac{1}{J} - \delta\Pi[h(y^a, x)] \right] |\phi_n^a|^2. \quad (41)$$

Here similarly to Eq. (26)

$$\delta\Pi(h) = \left[\frac{\pi}{2} \left(\frac{1}{\cosh(\beta h)} - 1 \right) + O\left(\frac{h^2}{T\epsilon_F}\right) \right]. \quad (42)$$

Finally, performing the Gaussian average over the ϕ fields and taking the limit $n \rightarrow 0$ one obtains the free energy

$$\beta\mathcal{F}(\bar{q}, q) = \frac{1}{4} z(\beta I)^2 (\bar{q}^2 - q^2) - \int_x^G \ln \left(\int_y^G 2 \cosh[\beta h(y, x)] / \{1 - J\Pi[0, h(y, x)]\} \right). \quad (43)$$

Corrected equations for q and \bar{q} are determined from the conditions $\partial\mathcal{F}(\bar{q}, q)/\partial\bar{q} = 0$, $\partial\mathcal{F}(\bar{q}, q)/\partial q = 0$. These are

$$\frac{1}{2}z(\beta I)^2\tilde{q} = \int_x^G \frac{\partial \ln C}{\partial \tilde{q}}, \quad \frac{1}{2}z(\beta I)^2q = - \int_x^G \frac{\partial \ln C}{\partial q},$$

$$C = \int_y^G 2 \cosh[\beta h(y,x)] / \{1 - J\Pi[0,h(y,x)]\}. \quad (44)$$

Under the condition $h(y,x) \leq 1$ a useful approximate equation for C is obtained:⁴⁵

$$\ln[CC(x,\tilde{q},q)] = -\frac{1}{2}\ln[1 + \gamma u^2(\tilde{q} - q)]$$

$$+ \frac{u^2}{2} \frac{[\tilde{q} - q(1 + \gamma x^2)]}{1 + \gamma u^2(\tilde{q} - q)}$$

$$+ \ln \left[\cosh \left(\frac{ux\sqrt{q}}{1 + \gamma u^2(\tilde{q} - q)} \right) \right]. \quad (45)$$

Here the following shorthand notations are used: $u = \beta I \sqrt{z}$, $C = J/\epsilon_f \ln(T/T_K)$ and $\gamma = 2c/\ln(T/T_K)$ with $c = (\pi/4 + 2/\pi^2) \sim 1$. We note again that when $J=0$, which corresponds to the absence of Kondo interaction, $C(x,\tilde{q},q) = 2 \exp[\frac{1}{2}z(\beta I)^2(\tilde{q} - q)] \cosh(\beta I x \sqrt{z} q)$, and Eq. (44) turns into the standard EA equation, providing, e.g., an exact identity $\tilde{q} = 1$.

In the vicinity of the freezing point Eq. (44) acquires the form

$$\tilde{q} = 1 - \frac{2c}{\ln(T/T_K)} - O\left(\frac{1}{\ln^2(T/T_K)}\right),$$

$$q = \int_x^G \tanh^2 \left(\frac{\beta I x \sqrt{z} q}{1 + 2cz(\beta I)^2(\tilde{q} - q)/\ln(T/T_K)} \right)$$

$$+ O\left(\frac{q}{\ln^2(T/T_K)}\right). \quad (46)$$

As a result of the numerical solution of Eqs. (46) we obtain the analog of Doniach's diagram for a disordered KL where the spin-glass freezing temperatures without and with Kondo screening contributions are shown ($T_f^{(0)}$ and T_f , respectively).

Here $T_f^{(0)}$ is obtained from the GL equation (40) neglecting the Kondo screening effect, and T_f was defined from Eqs. (46) under additional condition $\partial^2 \mathcal{F}_{sg} / \partial q^2 = 0$. The influence of Kondo screening on the diagonal element of the Parisi matrix \tilde{q} is illustrated by the inset of Fig. 3 (the bare value of $\tilde{q} = 1$ is shown by the dashed line). Like in the case of a perfect KL, the screening effect is noticeable when $T_f^{(0)} \sim T_K^{(0)}$.

The influence of the SG transition on a Kondo temperature for a KL with SG freezing was studied recently in Ref. 49. Although the Kondo effect in this paper is considered in a mean-field approximation (i.e., Kondo screening is treated as a true phase transition) and a static ansatz was applied for

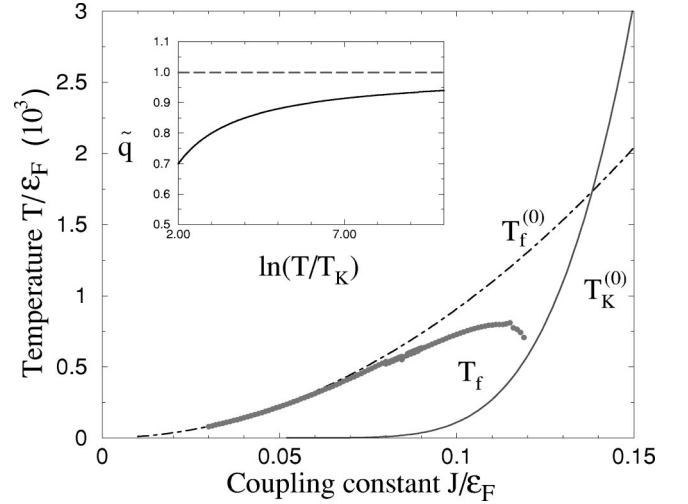


FIG. 3. Doniach's diagram for spin-glass transition in a disordered KL (see text for explanation).

SG, the authors obtained strong reduction of Kondo temperature in the same region $T_K \sim T_f^{(0)}$.

V. CORRELATIONS IN THE KONDO LATTICE BEYOND THE MEAN FIELD

The mean-field Doniach's diagram even in its improved form oversimplifies enormously the real picture of the interplay between three competing modes in the effective action (12). First of all, the proximity of three characteristic temperatures, T_K , T_{sl} , and T_N means that even when one of them is dominant, i.e., determines the local minimum of the free energy, two others define the fluctuations around the saddle point. Second, it is clear physically that only the Néel temperature T_N is a temperature of a *real* phase transition, whereas T_{sl} and T_K are merely characteristic crossover temperatures. The main shortcoming of the mean-field approximation is that this approach treats all three modes on equal footing. The method described in the preceding section allows one to get rid of the artificial phase transition at $T = T_K$, however, the problems with the description of the SL phase still exist. Meanwhile, it is known that the mean-field approximation for the SL state violates the local gauge invariance^{23,28,27,50} and fixes the phase θ of the SL mode W (17). The second-order phase transition from paramagnetic to the SL state³⁴ is an undesirable corollary of this crude approximation, and fluctuation corrections to the mean-field solution cannot improve this defect of the theory.

In this section we consider several scenarios of mode-mode correlations in a system described by the general equations (9) and (12) for the effective action \mathcal{A} . First, we offer the description of a *crossover* to a SL state, which allows one to bypass the mean-field saddle point (23). It will be demonstrated that the interplay between fluctuations of the fields ϕ and \mathbf{Y}_Q can trigger the transformation of localized critical relaxation AFM modes into SL-type correlations without loss of criticality. The main idea of our scenarios is that the heavy fermion state of KL is, in fact, an unconventional AFM state with spin excitations changing their character from Bose-like

spin fluctuations or spin waves to Fermi-like spinon modes. Next, we consider the behavior of the Kondo mode below T_{sl} and describe the quenching of Kondo scattering by SL fluctuations in a hatched part of Doniach's diagram (Fig. 2) where the static molecular field is absent.

We demonstrated above that the Kondo screening enhances SL correlations on a level of the mean-field approximation. A similar effect should exist on a more refined level of interacting fluctuation modes. To find the corresponding mechanism we refrain from the use of the bilocal representation of the spin mode. Instead of introducing the mode W associated with the gauge noninvariant $U(1)$ field described by the phase θ in Eq. (17), we consider the effect of interference of Kondo screening modes associated with spins located on different sites of the KL. In fact we consider the high-temperature precursors of the orthogonality catastrophe mentioned by Nozieres in his formulation of the "exhaustion problem."⁵¹ In a revised scheme we start with the action determined by the Hamiltonian (1). Starting with the integration over "fast" electronic variables (with energies $\sim \varepsilon_F$), we obtain

$$\begin{aligned} \mathcal{A}_{int} = & -\frac{2}{\bar{J}} \text{Tr} |\phi|^2 - \text{Tr} \frac{1}{I_{\mathbf{q}}} \mathbf{Y}_{\mathbf{q}} \mathbf{Y}_{-\mathbf{q}} - \text{Tr} \bar{f}_{j\sigma} \phi_j G_0(\mathbf{r}) \bar{\phi}_l f_{l\sigma} \\ & - \text{Tr} \bar{\phi}_j \phi_l \Pi_4 \bar{\phi}_l \phi_j - \text{Tr} \mathbf{Y}_j \bar{\phi}_j \phi_l \Pi_6 \bar{\phi}_l \phi_j \mathbf{Y}_l. \end{aligned} \quad (47)$$

Here instead of introducing the scalar mode W we retained higher-order terms in the Kondo screening fields. These terms are illustrated by the diagrams in Fig. 4.

The diagram in Fig. 4(a) describes the interference of Kondo clouds around the sites \mathbf{R}_j and \mathbf{R}_l . Zigzag lines stand for the AFM vector mode. Like all screening diagrams in Fermi systems it contains a Friedel-like oscillating factor. To estimate the polarization operator we use the asymptotic form of the electron Green's function in d dimensions at large distances,^{32,38}

$$\begin{aligned} G(r, \Omega) \sim & \frac{1}{(p_{Fr})^{(d-1)/2}} \exp \left[-\frac{|\Omega|}{2\varepsilon_F} p_{Fr} \right. \\ & \left. + i \left(p_{Fr} - \pi \frac{d+1}{4} \right) \text{sgn } \Omega \right]. \end{aligned} \quad (48)$$

Inserting this function in a four-tail diagram of Fig. 4(a), one comes to

$$\Pi_4 \sim -\frac{1}{T\varepsilon_F^2} \frac{\cos \left[2p_{Fr} - (d+1) \frac{\pi}{2} \right]}{(2p_{Fr})^{d-1}} + O \left(\frac{1}{\varepsilon_F^3} \ln \left[\frac{T}{\varepsilon_F} \right] \right). \quad (49)$$

Therefore we expect that this interference correlates with RKKY-type magnetic order, and the interaction between the corresponding modes represented by the diagram (b) in Fig. 4 influences the magnetic response in a "critical" region of the Doniach's diagram. This response is determined by the fluctuation corrections to Néel effective action,

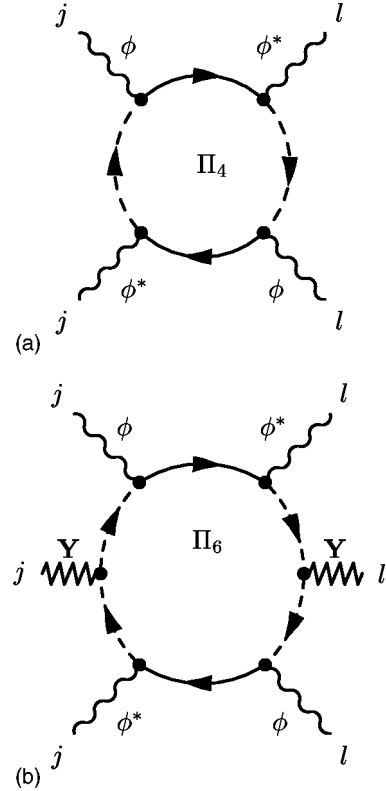


FIG. 4. Diagrams for fourth- and sixth-order polarization operators Π_4 (a) and Π_6 (b) in the effective action responsible for mode-mode coupling.

$$\delta \mathcal{A}_{eff} = \frac{1}{4} \sum_{\mathbf{q}, \alpha, \omega_n} Y^\alpha(\mathbf{q}, \omega_n) [I^{-1}(\mathbf{q}) + \chi_0 \delta_{n,0}] Y^\alpha(\mathbf{q}, \omega_n). \quad (50)$$

Here α are Cartesian coordinates, $\chi_0 = \beta/4$ is a static Curie susceptibility of an isolated spin $S=1/2$ [Fig. 5(a)]. The term in square brackets is, in fact, the inverse Ornstein-Zernicke correlator $\sim a_0^2(\mathbf{Q}-\mathbf{q})^2 + \tau_N$ at $T \geq T_N$ and $\mathbf{Q}-\mathbf{q} \rightarrow 0$. The first nonvanishing correction to χ_0 is given by Fig. 5(b). In this diagram the spins S_j and S_l are screened independently, (the wavy lines represent all parquet vertex insertions). In the mean-field approach the similar effects are de-

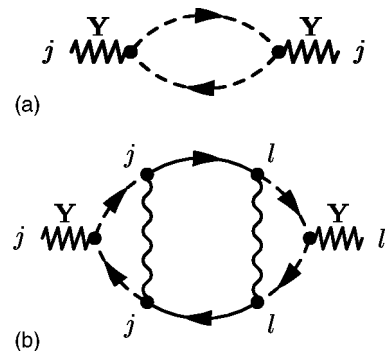


FIG. 5. Diagrams describing local (Curie-type) magnetic susceptibility χ_0 (a) and nonlocal correction taking into account Kondo screening of vertices (b).

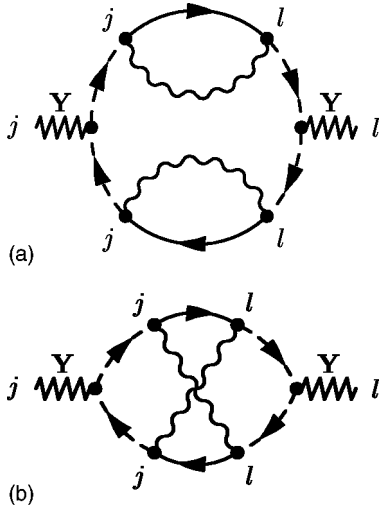


FIG. 6. Leading diagrams describing interference of Kondo clouds in magnetic susceptibility (see text for details).

scribed by Eq. (28). Indeed, each vertex correction $\Gamma_{i=j,l}(\omega, \epsilon) \sim \langle \phi(\epsilon) \bar{\phi}(\epsilon) \rangle$ gives the contribution $\sim 1/\ln(\epsilon/T_K)$, and integration over the internal frequency ϵ results in the $1/\ln(T_N^0/T_K)$ correction in Eq. (28).^{24,32}

The effects essentially beyond mean field are described by those diagrams that cannot be cut along a pair of electron propagators (solid lines) [see Figs. 6 and 7(a)]. The first of these diagrams [Fig. 6(a)] can be treated as a nonlocal correction to the one site spin susceptibility [Fig. 5(a)] induced by interfering flow and counterflow of two Kondo clouds. As a result, the spin-fermion propagator becomes nonlocal without introducing the mean-field order parameter (17). The next diagram [Fig. 6(b)] is a kind of “exchange” by these clouds in the course of two-spinon propagation. Up to now we exploited the “proximity” effects $T \gtrsim T_K$. A critical AFM mode given by the Fourier transform of the diagram of Fig.

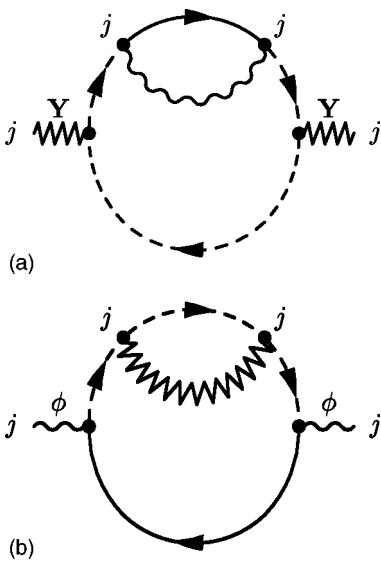


FIG. 7. (a) Next to parquet approximation for Kondo corrections to the magnetic susceptibility; (b) magnetic fluctuation correction to single-site Kondo scattering.

5(a) with the wave vector $\mathbf{q} \approx \mathbf{Q}$ also exists in this temperature interval, and, moreover, this mode is dominant in the spin susceptibility at $T \gtrsim T_N$. This means that the nonlocal contributions of Fig. 6 should be taken also at these \mathbf{q} . Due to nonlocality, the temperature dependence of the spin polarization loop will be weaker than the Curie law $1/T$, and the inverse static susceptibility given by these diagrams is

$$\chi_{\mathbf{Q}}^{-1}(T) = \chi_0^{-1}(T) + \chi_{sl}^{-1}(T) + \tilde{T}_{\mathbf{Q}}. \quad (51)$$

This deviation from the Curie law results in a depression of the Néel phase transition or, in other words, in extension of critical regime to temperatures well below T_N^0 in accordance with the scenario described in Ref. 28. Magnetic instabilities that can emerge at $T \ll T_N^0$ will be the instabilities of the spin liquid phase. These instabilities have much in common with itinerant fluctuational magnetism considered, e.g., in Refs. 52 and 53.

Diagram (a) in Fig. 7 with bare spinon propagators gives only a local correction to the susceptibility, however at $T \ll T_N^0$ where the spinon lines are dressed by the self-energies shown in Fig. 6(a), this diagram also becomes nonlocal and, therefore contributes to the nonlocal term on the right-hand side of Eq. (51). The processes taken into account in diagram (b) of Fig. 7 describe the feedback influence of spin fluctuations on the Kondo screening. This diagram together with higher-order terms of the same type results in the dynamical suppression of T_K as a result of the appearance of spin fluctuation energy $\omega_{sf} \sim \xi^{-z}$ in the logarithmic Kondo contribution $\ln(\epsilon_F/\max\{T, \omega_{sf}\})$. This mechanism is effective not too close to the real T_N where the magnetic correlation length ξ determining the short-range magnetic order is still comparable with the lattice spacing (here z is the dynamical critical exponent).

This schematic description is only a scenario of the theory of critical phenomena in KL's. The discussion of fluctuations around the SG transitions are beyond the scope of this paper. Some details of modulated replica symmetry breaking schemes, which combine treelike and wavelike structures in AFM SG may be found in Ref. 41. A more detailed calculation of the critical magnetic and spin-glass fluctuations in the spin liquid will be published separately.

VI. CONCLUDING REMARKS

We derived in this paper the phase diagram for the Kondo lattice model, starting with a high-temperature expansion of the effective action. As a first step, we succeeded in getting rid of one of the fictitious saddle points, i.e., we avoided the introduction of “Kondo-condensate” averages $\langle c_{k\sigma}^\dagger f_{i\sigma} \rangle$ used in previous revisions of the Doniach's diagram.^{25,25} In our modified Doniach's diagram (Fig. 3) the *renormalized* T_K is the lowest of all characteristic temperatures for all reasonable values of coupling constant α where one can neglect valence fluctuations. In fact, the mean-field calculations of Ref. 25 give a similar picture. The feedback of this result is that the strong Kondo regime is unachievable in a critical region of Doniach's diagram, and the real role of Kondo screening for small α where $T_N > T_{sl} > T_K$ is to reduce localized magnetic

moments and enhance the electronic density of states around ε_F . Thus the moderately heavy fermion systems with relatively big magnetic moments ordered antiferromagnetically arise (CeIn₃, CeAl₂ are possible examples).⁵⁴

In a critical region of Doniach's diagram Kondo screening changes radically the behavior of KL. According to our mean-field results the conventional AFM order is suppressed at $T \sim T_{sl} \geq T_N$. The SL phase that arises instead is, nevertheless, close to magnetic instability, and one can expect that the spin subsystem eventually orders magnetically. If the new transition temperature \tilde{T}_N is finite the singlet spinon coupling is incomplete, so that RVB's have residual magnetic moments, and these moments are ordered at $T = \tilde{T}_N$ (we emphasize once more that T_N marked by light circles in a hatched region of the phase diagram of Fig. 3 is not a real transition temperature. It rather designates the temperature region where critical AFM fluctuations arise). Of course, the magnitude of these moments is extremely small, and one can qualify this type of magnetic order as intermediate between localized and itinerant AFM. In the temperature interval $\tilde{T}_N < T < T_N$ the critical AFM relaxation mode characterizes the magnetic response of the system. When $\tilde{T}_N = 0$, one deals with a quantum phase transition, and the case $\tilde{T}_N < 0$, apparently, corresponds to short-range correlations existing in a wide temperature interval $0 < T < T_N$. This picture describes in gross features the magnetic properties of magnetic KL's, but any kind of quantitative description will be possible only after realization of the scenarios for the critical behavior of spin liquid briefly sketched in Sec. V.

Now we turn to the discussion of conclusions that could be derived from our theory concerning the nature of the heavy fermion state. The most important one is that the separation of charge and spin degrees of freedom existing in KL at high temperatures takes place also in a strong-coupling regime at $T \ll T_K$. Indeed, at high T exceeding all characteristic temperatures in the KL the spin excitation spectrum is simple structureless peak of the width T around zero energy. This peak is manifested as Curie-type magnetic susceptibility and trivial high-temperature corrections $\sim 1/T^n$ to all thermodynamic quantities due to weak paramagnetic spin scattering of the conduction electrons, whose Fermi-liquid continuum exists as independent charge branch of the elementary excitations. Since all transformations of the spin subsystem occur at $T > T_K$ (at least in a region of $\alpha < 0.2$ where the valence fluctuations are still negligible), this central peak still exists in a strong-coupling regime. Below $T_{sl} \sim T_K$ this peak is formed by spin liquid excitations. The character of these excitations resembles relaxation modes in a picture of fluctuation itinerant magnetism^{52,53} in a wide temperature interval down to T_{coh} where the coherent spin liquid regime of Fermi type is established. The interaction between the SL mode and the conduction electrons is the same exchange-type scattering as at high temperatures. This coupling constant \tilde{J} is, however, enhanced by the Kondo effect [see Eq. (25)]. The electrons in a layer of the width T_K around the Fermi level interact nonadiabatically with spin fermions at low T . As a result the giant Migdal effect arises⁵⁵ which results in a

strong electron mass enhancement. So, the heavy fermion state in accordance with this picture is a two-component Fermi liquid where the characteristic energies of the charge subsystem (slow electrons with $\epsilon < T_K$) and the spin subsystem (spinons with $\omega \sim T_{sl}$) are nearly the same.

An exponentially narrow low-energy peak of predominantly spin origin appears practically in all theories of strongly correlated electron systems. In the archetypal Hubbard model this peak arises on the dielectric side of Mott-Hubbard transition, and still exists on the metallic side, where the charge and spin degrees of freedom are already coupled. This is the point where the links between Hubbard and Anderson models arise at least on a level of dynamical mean-field theory (DMFT) valid at $d \rightarrow \infty$.⁵⁶ On the other hand, the mean-field solution that results in merged charge and spin degrees of freedom in a central peak becomes exact in the large- N theories for the $N = \infty$ saddle point.⁵⁷ Recent achievements in this direction are connected with confirmation of Noziere's prediction of a second scale in the Kondo lattice⁵¹ in the limit of the exhaustion regime of small electron concentration. At this temperature the "bachelor" spins form a coherent Fermi liquid and lose their localized nature. This anticipation was confirmed by recent calculations within the mean-field slave boson approximation of $N \rightarrow \infty$ theory.⁵⁸ In our approach the regime of bachelor spins does not arise, because the Kondo coupling remains weak even at $T \ll T_K$ (see above), but the spin degrees of freedom become coherent at $T \sim T_{coh}$, so that the existence of two coherence scales is an intrinsic property of the model.

Another aspect of large N theories is the possibility of supersymmetric description that allows combined description of spin degrees of freedom in a mixed fermion-boson $SU(N)$ representation.⁵⁹ This approach allowed the authors to retain intersite RKKY interaction in the limit of $N \rightarrow \infty$ in spite of $1/N^2$ effect of suppression of all intersite magnetic correlations in a standard large N approach. The use of the Popov-Fedotov representation allows the treatment of different magnetic modes described by these operators as semifermions or semibosons in different physical situations.³³ In this paper we appealed to $SU(2)$ symmetry. The general recipe of generation of modes with intermediate statistics between Fermi and Bose limiting cases for the $SU(N)$ algebra is offered in Ref. 60. In fact, the eventual transformation of the states with intermediate statistics into true fermions (bosons) occurs only at $T \rightarrow 0$. Thus this approach may be extremely useful for an adequate description of quantum phase transitions.⁶¹

In principle, other collective modes can modify the scenario of the AFM phase transition in KL's. In particular, the low-lying crystal-field excitations may intervene the magnetic phase transition in the same fashion as Kondo clouds in our theory. Probably the CeNiSn family of semimetallic Kondo lattices is an example of such an intervention.⁶²

ACKNOWLEDGMENTS

Authors thank A. Mishchenko for fruitful collaboration in the early stages of this work, A. Luther, D. Aristov, and G. Khaliullin for valuable discussions, and A. Tselvik for useful

remarks. The work was supported by SFB-410. M.K. acknowledges the support of the Alexander von Humboldt Foundation, K.K. is grateful to Israeli-USA BSF-1999354 for partial support and to the University of Würzburg for hospitality.

APPENDIX A:

To evaluate the contribution of the Kondo mode in the expansion (20) for the effective action, one needs the Fourier transform of the Green's function K_ϕ (19). This is

$$\begin{pmatrix} \bar{\phi}_n(\mathbf{k})G^0(\mathbf{q})\phi_n(\mathbf{k}) & 0 & \bar{\phi}_n(\mathbf{k})G^0(\mathbf{q})\phi_n(\mathbf{k}+\mathbf{Q}) & 0 \\ 0 & \bar{\phi}_n(\mathbf{k})G^0(\mathbf{q})\phi_n(\mathbf{k}) & 0 & \bar{\phi}_n(\mathbf{k})G^0(\mathbf{q})\phi_n(\mathbf{k}+\mathbf{Q}) \\ \bar{\phi}_n(\mathbf{k}+\mathbf{Q})G^0(\mathbf{q})\phi_n(\mathbf{k}) & 0 & \bar{\phi}_n(\mathbf{k}+\mathbf{Q})G^0(\mathbf{q})\phi_n(\mathbf{k}+\mathbf{Q}) & 0 \\ 0 & \bar{\phi}_n(\mathbf{k}+\mathbf{Q})G^0(\mathbf{q})\phi_n(\mathbf{k}) & 0 & \bar{\phi}_n(\mathbf{k}+\mathbf{Q})G^0(\mathbf{q})\phi_n(\mathbf{k}+\mathbf{Q}) \end{pmatrix} \quad (\text{A1})$$

The components $D_{m\sigma}(\mathbf{q})$ of the semi-Fermionic Green's function D in Eq. (20) are determined by inverting the matrix (18). There are normal and anomalous components,

$$-\int_0^\beta d\tau e^{i\omega_m\tau} \langle T_\pi f_\sigma(\mathbf{q},\tau) \bar{f}_\sigma(\mathbf{q},0) \rangle = \frac{i\omega_m - W_{\mathbf{q}}}{(i\omega_m - W_{\mathbf{q}})^2 - Y^2} \quad (\text{A2})$$

and

$$-\int_0^\beta d\tau e^{i\omega_m\tau} \langle T_\pi f_\sigma(\mathbf{q},\tau) \bar{f}_\sigma(\mathbf{q}+\mathbf{Q},0) \rangle = \frac{Y \hat{\tau}_{\sigma\sigma}^z}{(i\omega_m - W_{\mathbf{q}})^2 - Y^2}, \quad (\text{A3})$$

respectively. Here $Y = \mathcal{N}I_{\mathbf{Q}}/2$ and $W_{\mathbf{q}} = I_{\mathbf{q}}\Delta$.

To perform calculations in real space, one should know the inverse Green's function (13) in coordinate representation:

$$D_m^{-1}(W, \mathbf{Y}) = \begin{pmatrix} i\omega_m + Y_j^z & Y_j^+ & W_{jl} & 0 \\ Y_j^- & i\omega_m - Y_j^z & 0 & W_{jl} \\ W_{lj} & 0 & i\omega_m - Y_l^z & Y_l^+ \\ 0 & W_{lj} & Y_l^- & i\omega_m + Y_l^z \end{pmatrix}. \quad (\text{A4})$$

It should be noted that the nonlocal term W_{jl} in Eq. (A4) responsible for SL correlations transforms into diagonal term $W_{\mathbf{q}}$ in momentum representation (13), whereas the local staggered field \mathbf{Y}_i has nondiagonal matrix elements in momentum space corresponding to AFM correlations at $\mathbf{q} = \mathbf{Q}$.

APPENDIX B:

The sum of polarization integrals presented in Fig. 1 is given by the following equation:

$$\Pi_n(Y, W_{\mathbf{q}}) = -T \sum_{m,\sigma,\mathbf{p}} D_{m\sigma}(\mathbf{p}) G_{m+n}^0(\mathbf{p}+\mathbf{q}) \quad (\text{B1})$$

Only the normal component (A2) survives in this equation as a result of spin summation. The Neel loop [Fig. 1(a)] after performing frequency summation acquires the form

$$\begin{aligned} \Pi(Y,0) = \sum_{\mathbf{p}} \left\{ \tanh\left(\frac{\xi_{\mathbf{p}}}{2T}\right) \left[\frac{\xi_{\mathbf{p}} - Y}{(\xi_{\mathbf{p}} - Y)^2 + \lambda^2} + \frac{\xi_{\mathbf{p}} + Y}{(\xi_{\mathbf{p}} + Y)^2 + \lambda^2} \right] \right. \\ \left. + \frac{\lambda}{\cosh(Y/T)} \left[\frac{1}{(\xi_{\mathbf{p}} - Y)^2 + \lambda^2} + \frac{1}{(\xi_{\mathbf{p}} + Y)^2 + \lambda^2} \right] \right. \\ \left. - \tanh\left(\frac{Y}{T}\right) \left[\frac{\xi_{\mathbf{p}} - Y}{(\xi_{\mathbf{p}} - Y)^2 + \lambda^2} - \frac{\xi_{\mathbf{p}} + Y}{(\xi_{\mathbf{p}} + Y)^2 + \lambda^2} \right] \right\}. \quad (\text{B2}) \end{aligned}$$

Here $\xi_p = \varepsilon_p - \varepsilon_F$, $\lambda = \pi T/2$. This integral is an even function of the order parameter, $\Pi(Y) = \Pi(-Y)$. Using the inequality $Y \ll \varepsilon_F$, two last terms can be simplified, and introducing the integral over the electron band with constant density of states ρ_0 , one has

$$\begin{aligned} \Pi(Y,0) = \frac{1}{4} \rho_0 \int_{-\varepsilon_F}^{\varepsilon_F} d\xi \left\{ \tanh\left(\frac{\xi_{\mathbf{p}}}{2T}\right) \right. \\ \left. \times \left[\frac{\xi_{\mathbf{p}} - Y}{(\xi_{\mathbf{p}} - Y)^2 + \lambda^2} + \frac{\xi_{\mathbf{p}} + Y}{(\xi_{\mathbf{p}} + Y)^2 + \lambda^2} \right] \right\} \\ \left. + \frac{\pi \rho_0}{2 \cosh(Y/T)} + \frac{\rho_0 Y}{\varepsilon_F} \tanh\left(\frac{Y}{T}\right). \quad (\text{B3}) \end{aligned}$$

Incorporating ρ_0 in dimensionless variables, one has in the vicinity of the Néel point where $Y \ll T$,

$$\Pi(Y,0) = \frac{1}{2} \left[\ln \left(\frac{\epsilon_F^2}{4T^2} \right) + \pi \right] - a_N \left(\frac{Y}{T} \right)^2 + O \left(\frac{Y^2}{T\epsilon_F} \right). \quad (\text{B4})$$

The logarithmic term is, in fact, included in the renormalized coupling constant \tilde{J} in Eq. (25) for the effective action, and the remaining terms give Eq. (26) for $\delta\Pi$. Deeper in the magnetic phase where $Y \gg T$, the Kondo effect is quenched by the molecular field, so that

$$\Pi = \ln \left(\frac{\epsilon_F}{Y} \right) + b_N \left(\frac{T}{Y} \right)^2 + O \left(\frac{T^2}{\epsilon_F^2} \right). \quad (\text{B5})$$

The numerical coefficients a_N, b_N arising from approximate estimates of the integrals in Eq. (A3) are of the order of unity.

The SL loop [Fig. 1(b)] can be estimated for $\mathbf{q}=0$. After frequency summation it is presented by the following integral:

$$\begin{aligned} \Pi(0,\Delta) &= \frac{1}{2} \sum_{\mathbf{p}} \frac{\xi_{\mathbf{p}} \tanh \left(\frac{\xi_{\mathbf{p}}}{2T} \right) + I_{\mathbf{p}} \Delta \tanh \left(\frac{I_{\mathbf{p}} \Delta}{T} \right) + \frac{\lambda}{2 \cosh(I_{\mathbf{p}} \Delta / T)}}{\xi_{\mathbf{p}}^2 + \lambda^2}. \end{aligned} \quad (\text{B6})$$

This function is also even, $\Pi(\Delta) = \Pi(-\Delta)$. Extracting from Eq. (B6) the logarithmic term $\ln(\epsilon_F/2T)$, one comes to Eq. (30) for $\delta\Pi$. In a critical region of Doniach's diagram where $\Delta \ll T$, one has

$$\delta\Pi(0,\Delta) = a_{sl} \frac{\Delta^2}{2T^2} \sum_{\mathbf{p}} \frac{v_{\mathbf{p}}^2}{\xi_{\mathbf{p}}^2 + \lambda^2}, \quad a_{sl} \sim 1. \quad (\text{B7})$$

-
- ¹G.G. Lonzarich, J. Magn. Magn. Mater. **76-77**, 1 (1988); M. Springford, Physica B **171**, 151 (1990); Y. Onuki and A. Hasegawa, J. Magn. Magn. Mater. **108**, 19 (1992).
- ²M. Sigrist and K. Ueda, Rev. Mod. Phys. **63**, 239 (1991); R.H. Heffner and M.R. Norman, Comments Condens. Matter Phys. **17**, 361 (1996).
- ³U. Rauchschwalbe, Physica B **147**, 1 (1987); H. R. Ott, in *Progress in Low Temperature Physics*, edited by D. F. Brewer (Elsevier, Amsterdam, 1987) Vol. XI, p. 215; N. Grewe and F. Steglich, in *Handbook on the Physics and Chemistry of Rare Earths*, edited by K. A. Gschneider, Jr. and L. Eyring (Elsevier, Amsterdam, 1991), Vol. 14, p. 343.
- ⁴J.M. Effantin, J. Rossat-Mignod, P. Burllet, H. Bartholin, S. Kunii, and T. Kasuya, J. Magn. Magn. Mater. **47-48**, 145 (1985).
- ⁵A. Loidl, A. Krimmel, K. Knorr, G. Sparr, M. Lang, C. Geibel, S. Horn, A. Grauel, F. Steglich, B. Welslau, N. Grewe, H. Nakotte, F. de Boer, and A.P. Murani, Ann. Phys. (Leipzig) **1**, 78 (1992); A. Bernasconi, M. Mombelli, Z. Fisk, and H.R. Ott, Z. Phys. B: Condens. Matter **94**, 423 (1994).
- ⁶A. de Visser and J.J.M. France, J. Magn. Magn. Mater. **100**, 204 (1991).
- ⁷H. von Löhneysen, A. Neubert, T. Pietrus, A. Schröder, O. Stockert, U. Tutsch, M. Löwenhaupt, A. Rosch, and P. Wölfle, Eur. Phys. J. B **5**, 447 (1998).
- ⁸A. de Visser, M.J. Graf, P. Estrela, A. Amato, C. Baines, D. Andreica, F.N. Gyax, and A. Schenk, Phys. Rev. Lett. **85**, 3005 (2000).
- ⁹J. Rossat-Mignod, L.P. Regnault, J.L. Jacoud, C. Vettier, P. Lejay, J. Flouquet, E. Walker, D. Jaccard, and A. Amato, J. Magn. Magn. Mater. **76&77**, 376 (1988).
- ¹⁰N.D. Mathur, F.M. Groschke, S.R. Julian, J.R. Walker, D.M. Fr-eye, R.K.W. Haselwimmer, and G.G. Lonzarich, Nature (London) **394**, 39 (1998).
- ¹¹C. M. Varma, in *Theory of Heavy Fermions and Valence Fluctuations*, Springer Series in Solid State Sciences Vol. 62, edited by T. Kasuya and T. Saso (Springer, Berlin, 1985), p. 277.
- ¹²Yu. Kagan, K.A. Kikoin, and N.V. Prokof'ev, Physica B **182**, 201 (1992).
- ¹³M.B. Maple, M.C. de Andrade, J. Herrmann, Y. Dalichaouch, D.A. Gajewski, C.L. Seaman, R. Chau, R. Movshovich, M.C. Aronson, and R. Osborn, J. Low Temp. Phys. **99**, 314 (1995).
- ¹⁴L.Z. Liu, J.W. Allen, C.L. Seaman, M.B. Maple, Y. Dalichaouch, J.S. Kang, M.S. Torikachvili, and M.A. Lopez de la Torre, Phys. Rev. Lett. **68**, 1034 (1992).
- ¹⁵S. Süllow, G.J. Nieuwenhuys, A.A. Menovsky, J.A. Mydosh, S.A.M. Mentink, T.E. Mason, and W.J.L. Buyers, Phys. Rev. Lett. **78**, 354 (1997).
- ¹⁶B. Becker, S. Ramakrishnan, A.A. Menovsky, G.J. Nieuwenhuys, and J.A. Mydosh, Phys. Rev. Lett. **78**, 1347 (1997).
- ¹⁷D.X. Li, Y. Shiokawa, Y. Homma, A. Uesawa, A. Dönni, T. Suzuki, Y. Haga, E. Yamamoto, T. Homma, and Y. Onuki, Phys. Rev. B **57**, 7434 (1998).
- ¹⁸O.O. Bernal, D.E. MacLaughlin, H.G. Lukefahr, and A. Andraka, Phys. Rev. Lett. **75**, 2023 (1995).
- ¹⁹J.C. Gomez Sal, J. Garcia Soldevilla, J.A. Blanco, J.I. Espeso, J. Rodriguez Fernandez, F. Luis, F. Bartolome, and J. Bartolome, Phys. Rev. B **56**, 11 747 (1997).
- ²⁰J. Garcia Soldevilla, J.C. Gomez Sal, J.A. Blanco, J.I. Espeso, and J. Rodriguez Fernandez, Phys. Rev. B **61**, 6821 (2000).
- ²¹D. Eom, M. Ishikawa, J. Kitagawa, and N. Takeda, J. Phys. Soc. Jpn. **67**, 2495 (1998).
- ²²S. Doniach, Physica B **91**, 231 (1977); C. Lacroix and M. Cyrot, Phys. Rev. B **20**, 1969 (1979).
- ²³P. Coleman and N. Andrei, J. Phys.: Condens. Matter **1**, 4057 (1989).
- ²⁴K.A. Kikoin, M.N. Kiselev, and A.S. Mishchenko, Pis'ma Zh. Eksp. Teor. Fiz. **60**, 583 (1994) [JETP Lett. **60**, 600 (1994)].
- ²⁵J.R. Iglesias, C. Lacroix, and B. Coqblin, Phys. Rev. B **56**, 11 820 (1997); B.H. Bernhard, C. Lacroix, J.R. Iglesias, and B. Coqblin, *ibid.* **61**, 441 (2000).
- ²⁶V.N. Popov and S.A. Fedotov, Zh. Eksp. Teor. Fiz. **94**, 183 (1988) [Sov. Phys. JETP **67**, 535 (1988)].

- ²⁷L.B. Ioffe and A.I. Larkin, Phys. Rev. B **39**, 8988 (1989); P.A. Lee and N. Nagaosa, *ibid.* **46**, 5621 (1992).
- ²⁸K.A. Kikoin, M.N. Kiselev, and A.S. Mishchenko, Physica B **230-232**, 490 (1997).
- ²⁹N. Read and D.M. Newns, J. Phys. C **16**, 3273 (1983).
- ³⁰F. Bouis and M.N. Kiselev, Physica B **259-261**, 195 (1999).
- ³¹M.N. Kiselev and R. Oppermann, Phys. Rev. Lett. **85**, 5631 (2000).
- ³²K.A. Kikoin, M.N. Kiselev, and A.S. Mishchenko, Zh. Eksp. Teor. Fiz. **112**, 729 (1997) [Sov. Phys. JETP **85**, 490 (1997)].
- ³³The specific feature of $S=1/2$ is that the set $2\pi T(m+1/4)$ can be interpreted both as a “semi-Fermionic” and a “semi-Bosonic” field. The complementary field ϕ which appears in the decoupling procedure for bi-Grassmann products in representation (8) will be referred to as a semi-Bosonic field for the physical reasons which are discussed below.
- ³⁴G. Baskaran, Z. Zou, and P.W. Anderson, Solid State Commun. **63**, 973 (1987); A. Ruckenstein, P. Hirschfeld, and J. Appel, Phys. Rev. B **36**, 857 (1987).
- ³⁵A.M. Tsvetlik and P. Wiegmann, Adv. Phys. **32**, 483 (1983).
- ³⁶A.A. Abrikosov and A.A. Migdal, J. Low Temp. Phys. **3**, 519 (1970).
- ³⁷A.Yu. Zyuzin and B.Z. Spivak, Pis'ma Zh. Eksp. Teor. Fiz. **43**, 185 (1986) [JETP Lett. **43**, 234 (1986)]; L.N. Bulayevskii and S.V. Panyukov, *ibid.* **43**, 190 (1986) [*ibid.* **43**, 240 (1986)].
- ³⁸D.N. Aristov, Phys. Rev. B **55**, 8064 (1996).
- ³⁹J. Stein, Eur. Phys. J. B **12**, 5 (1999).
- ⁴⁰S. Sachdev, N. Read, and R. Oppermann, Phys. Rev. B **52**, 10 286 (1995).
- ⁴¹R. Oppermann, D. Sherrington, and M. Kiselev, cond-mat/0106066 (unpublished).
- ⁴²A mean-field solution of a fully connected quantum Heisenberg SG model in a large N limit that involves the quantum dynamics of spin variables was presented in A. Georges, O. Parcollet, and S. Sachdev, Phys. Rev. Lett. **85**, 840 (2000).
- ⁴³A. Sengupta and A. Georges, Phys. Rev. B **52**, 10 295 (1995).
- ⁴⁴S.F. Edwards and P.W. Anderson, J. Phys. F: **5**, 965 (1975).
- ⁴⁵M.N. Kiselev and R. Oppermann, Pis'ma Zh. Eksp. Teor. Fiz. **71**, 359 (2000) [JETP Lett. **71**, 250 (2000)].
- ⁴⁶D. Sherrington and S. Kirkpatrick, Phys. Rev. Lett. **35**, 1972 (1975).
- ⁴⁷R. Oppermann and A. Muller-Groeling, Nucl. Phys. B **401**, 507 (1993).
- ⁴⁸K. Binder and A.P. Young, Rev. Mod. Phys. **58**, 801 (1986).
- ⁴⁹A. Theumann, B. Coqblin, S.G. Magalhães, and A.A. Schmidt, Phys. Rev. B **63**, 054409 (2001).
- ⁵⁰I. Affleck, Z. Zou, T. Hsu, and P.W. Anderson, Phys. Rev. B **38**, 745 (1988).
- ⁵¹P. Nozieres, Ann. Phys. (Paris) **10**, 19 (1985); Eur. Phys. J. B **6**, 447 (1998).
- ⁵²T. Moriya, *Spin Fluctuations in Itinerant Electron Magnetism* (Springer, Berlin, 1985).
- ⁵³Y. Okuno and K. Miyake, J. Phys. Soc. Jpn. **67**, 3342 (1998).
- ⁵⁴Metallic compounds containing U, apparently, should be described by the Anderson-lattice Hamiltonian because of the partially itinerant nature of the $5f$ electrons, so we refrain here from direct application of our model to U-based heavy fermion systems.
- ⁵⁵K. Kikoin, J. Phys.: Condens. Matter **8**, 3601 (1996).
- ⁵⁶A. Georges, G. Kotliar, W. Krauth, and M. Rozenberg, Rev. Mod. Phys. **68**, 13 (1996).
- ⁵⁷P. Coleman, Phys. Rev. B **35**, 5072 (1987).
- ⁵⁸S. Burdin, A. Georges, and D.R. Grempel, Phys. Rev. Lett. **85**, 1048 (2000).
- ⁵⁹P. Coleman, C. Pepin, and A.M. Tsvetlik, Phys. Rev. B **62**, 3852 (2000).
- ⁶⁰M. N. Kiselev, H. Fedmann, and R. Oppermann, Eur. Phys. J. B **22**, 53 (2001).
- ⁶¹A. M. Tsvetlik (private communication).
- ⁶²Yu.M. Kagan, K.A. Kikoin, and A.S. Mishchenko, Phys. Rev. B **55**, 12 348 (1997); K.A. Kikoin, M.N. Kiselev, A.S. Mishchenko, and A. de Visser, *ibid.* **59**, 15 070 (1999).